RSC Advances

ROYAL SOCIETY OF CHEMISTRY

www.rsc.org/advances

A naked-eye pH-modulated ratiometric photoluminescence sensor based on dual-emission quantum dot@silica nanoparticles for Zn^{2+} and IO_3^-

Yang Li [a1], Qiang Ma [a1], Guodong Li[b], Xingguang Su [a]*

[a] Department of Analytical Chemistry, College of Chemistry, Jilin University, Changchun, 130012, P.R. China

[b] State Key Laboratory of Inorganic Synthesis and Preparative Chemistry, College of Chemistry, Jilin University,Changchun,130012, P.R. China

*Corresponding author. Tel.: 086 431 85168352.

E-mail address: suxg@jlu.edu.cn (Xingguang Su).

1 These authors contributed equally to this work.

Abstract

In this paper, we developed a ratiometric photoluminescence (PL) sensor comprising dual-emission quantum dots (QDs)@silica nanoparticles for Zn^{2+} and IO_3^-. The PL signal of red-emitting QDs in the silica nanoparticles core worked as reference, while the PL signal of green-emitting QDs covalently linked onto the silica surface could be selectively quenched or restored by the analyte. After the PL quenching of green-emitting QDs by phenanthroline (Phen), Zn^{2+} can recover the PL under the alkaline condition via the formation of Zn-Phen complex in the solution. Besides, IO_3^- can interact with green-emitting QDs through oxidation-reduction reactions under the acidic condition, leading to the further PL quenching. Under the optimized conditions, linear relationships between the PL intensity ratio of ratiometric system and ion concentration were obtained from 5 to 100 μM for Zn^{2+} and from 5 to 150 μM for IO_3^-, respectively. The detection limits (LOD) of Zn^{2+} and IO_3^- were 1.15 and 1.76 μM, respectively. The proposed method was sensitive, high selective and intuitional. It has been successfully applied in the determination of Zn^{2+} and IO_3^- in the serum samples and table salt with satisfactory results.

Keywords: Ratiometric photoluminescence sensor; Dual-emission quantum dots; Zinc ions; Iodate ions

1. Introduction

Until now, a series of functional nanoparticles were utilized to establish various kinds of nanosensor systems, such as QDs, Au nanoparticles, Fe_3O_4 nanoparticles, carbon dots, etc.[1-3] Among them, QDs possess distinct optical properties, including broad excitation spectra, narrow emission peak, high quantum yields and resistance to photobleaching.[4] QDs with different sizes can emit different bands, affording the application of incorporating different-sized QDs in one nanosensor or nanoprobe. And the polychrome color changes provide convenience for the naked eye detection. QD-based fluorescence methods have been widely applied to the fluorescent labeling, biological imaging and sensing systems due to its simplicity, sensitivity, easy operation and low cost features. However, there are still two key questions in the development of QD-based PL sensors, the reliability and scope of application. On the one hand, most of the reported QD-based sensors were based on the quenching or enhancement of single PL signal. These single lumophore-based sensors tended to be compromised by some other factors, such as the instrumental efficiency and environmental fluctuations. On the other hand, QD-based PL sensing systems modified by different chemical methods have been extensively exploited in the quantitative determination of cations, especially the transition metal ions. But there are little reports about it for anion detection.[5] Therefore, designing a variety of more sensitive and reliable QD-based PL sensors suitable for cations and anions is of great significance.

In order to improve sensing reliability, ratiometric sensors have been proposed. Ratiometric PL sensors comprising two signal reporters have attracted increasing attention in recent years owing to its remarkable advantages.[6-7] In the ratiometric PL sensors systems, one signal transducer works as analyte-sensing, and the other signal reporter keeps stable signals as reference. Two

signal reporters get better measured response to the analyte by lessening out experimental fluctuations. So, the ratiometric PL sensors greatly improve the sensitivity and reliability at trace quantity levels via self-calibration of two or more different PL signals.[8-10] For example, a kind of silica nanobead-based ratiometric Cu^{2+} sensor was reported.[11] RBITC (response dye) was covalently linked on the surface of silica nanoparticles, and FITC (reference dye) was doped in the interior. The RBITC emission band decreased through quenching in the presence of Cu^{2+}, while the reference FITC was unaffected. In addition, we have designed a direct naked-eye colorimetric analysis of Hg^{2+} based on the bi-color QDs multilayer films.[12]

Zinc exists in the human body in the form of Zn^{2+}, and it is the second most abundant transition metal in the body.[13] Zn^{2+} serves as catalytic and structural cofactor affecting gene expression, neural related signal transmission, and facilitating enzyme regulation. Disorder of Zn^{2+} metabolism can result in various diseases, such as Alzheimer's disease, epilepsy and infantile diarrhea.[14-15] Iodine is the necessary trace element during growth of human body. The lack of iodine can lead to thyromegaly and impact on people's mental development at the same time. Long-term excessive iodine intake can also cause disease and affect the health of the body.[16-18] Introducing potassium iodate in the salt is the most simple and effective method to prevent iodine deficiency. So far, many PL sensors have been designed for Zn^{2+} or IO_3^- detection based on proteins, nanoparticles, rhodamine, fluorescein, quinoline derivatives, and so on.[19-22] And a number of Zn^{2+} ratiometric sensors have been proposed, such as polyethylenimine conjugated $[Ru(bpy)_3]^{2+}$@SiNPs ratiometric fluorescent nanoprobe, squaraine based ratiometric PL probe, tetrazolylpyridine-based ratiometric fluorescent chemosensor, phenylbenzimidazole derivative-based ratiometric PL probe, and so on.[23-26] Nevertheless, the ratiometric PL sensors

based on QDs for Zn^{2+} and IO_3^- in one system have been rarely reported.

In this work, we developed a novel kind of dual-emission QD@silica nanoparticles-based ratiometric PL sensor (QSR) for the detection of Zn^{2+} and IO_3^-. As shown in **Scheme 1**, QSR consisted of two different CdTe QDs, the red-emitting QDs were embedded in the core of silica nanoparticles, and the green-emitting QDs were covalently linked onto the silica surface. The red-emitting QDs in silica nanoparticles emitted stable red PL avoiding the interference of analyte, and relatively constant PL intensity served as internal reference to eliminate the instrument and surrounding environment interference. In the presence of Phen, the PL intensity of the green-emitting QDs was quenched via the electronic interaction between QDs and Phen, and the PL intensity ratio of the QSR decreased accordingly. Under the alkaline pH condition, the PL intensity of the green-emitting QDs can be recovered upon the addition of Zn^{2+} selectively. On the contrary, IO_3^- can continue to quench the PL intensity of the green-emitting QDs under acidic pH condition due to the oxidation-reduction reactions between IO_3^- and CdTe QDs. Therefore, QSR can detect Zn^{2+} and IO_3^- via the modulation of the pH with high sensitivity and selectivity.

2. Experimental section

2.1 Materials and apparatus

All chemical reagents were of analytical reagent grade and were used without further purification. Tellurium powder, $CdCl_2$, $NaBH_4$ and tetraethoxysilane (TEOS) were purchased from Aldrich Chemical Co. Mercaptosuccinic acid (MPA) was purchased from J&K Chemical Co. 1-ethyl-3-[3-dimethylaminopropyl] carbodiimide hydrochloride (EDC), N-hydroxysuccinimide (NHS), 3-mercaptopropyltrimethoxysilane (MPS) and 3-aminopropyltriethoxysilane (APTS) were purchased from Sigma-Aldrich Corporation. Phen, Ammonium hydroxide, $Zn(NO_3)_2 \cdot 6H_2O$, KIO_3,

NaCl and other chemicals used were obtained from Beijing Dingguo Biotechnology Co. Ltd. 10 mM phosphate buffer solution (PBS) of various pH values were prepared. The water used in all experiments had a resistivity higher than 18 MΩ cm^{-1}.

The Fluorescence experiments were performed on a RF-5301 PC spectrofluorophotometer (Shimadzu Co., Kyoto, Japan) equipped with a xenon lamp using right-angle geometry. A 1 cm path-length quartz cuvette was used during the measurements of the PL spectrum. ICP (OPTIMA 3300DV) was used as reference method for measuring serum Zinc. All pH measurements were made with a PHS-3C pH meter (Hangzhou, China,).

2.2 Synthesis of CdTe QDs

The CdTe QDs were synthesized by refluxing routes as described in previous method.[27] Briefly, the precursor Sodium hydrogen telluride (NaHTe) was produced in an aqueous solution by the reaction of sodium borohydride ($NaBH_4$) with Te powder at a molar ratio of 2:1. Then, 1.25 mM $CdCl_2$ solution at pH 11.4 and stabilizing agent MPA were added into a 250 mL three-necked flask under N_2 atmosphere. The molar ratio of Cd^{2+}/MPA/HTe^- was 1:2.4:0.5. The fresh precursor solution was injected to the $CdCl_2$ solution and the solution was subjected to a reflux at 100 ℃ under stirring and condenser conditions. Stable water-compatible MPA-capped CdTe QDs were obtained. The PL emission wavelengths of the green and red emissive CdTe QDs used in the present experiments were 555 nm and 654 nm. The concentrations of both QDs were 1 μM, respectively.

2.3 Preparation of QD@silica nanoparticles and surface modification

The QD@silica nanoparticles were synthesized by a modification process based on the Stöber method.[28-29] In a typical process, 15 mL of ultrapure water, 40 mL of ethanol, and 7 mL of

red-emitting CdTe QDs solution were mixed under stirring in a 100 mL flask for 10 min. The flask was coated with aluminum foil. 20 μL of MPS was added, and the mixed solution was stirred for 12 h. Then, 0.5 mL of TEOS and ammonium hydroxide were added successively into the solution, and the solution was stirred for another 12 h. Then, 100 μL of APTS was introduced into the above mixture to modify the silica surface with amino groups and stirred for another 12 h. After the reaction, the resulting silica nanoparticles embedded with red-emitting QDs were obtained by centrifuging and washed with ethanol and ultrapure water for several times to remove the unreacted chemicals. Ultimately, the amino-modified QD@silica nanoparticles were redispersed in 10 mL of ultrapure water and preserved for further experiments.

2.4 Preparation of dual-emission QD@silica nanoparticles-based ratiometric PL sensor (QSR)

0.5 mL of green-emitting QDs solution was dispersed in 1 mL H_2O in the flask. 2 mL of EDC/NHS (2 mg/mL) was added, and the solution was stirred for 15min. Then, 3 mL of the amino-modified QD@silica nanoparticles was introduced, and the mixture was stirred for 4 h in the dark. The resulting dual-emission silica nanoparticles were centrifuged and washed with ultrapure water for three times. The final product QSR was dispersed in 10 mL of ultrapure water for further use.

2.5 Photoluminescence assays

In the experiments, all PL spectra measurements were performed under the same conditions: the slit widths of the excitation and emission were 5 nm and 10 nm, and the excitation wavelength was set at 400 nm. The emission was scanned from 420 to 780 nm. In the PL "turn off" step, 20 μL of QSR and different concentrations of Phen solution were successively added into a 2.0 mL

calibrated test tube. The PL spectrum was measured and the corresponding PL intensity ratio was calculated. In the procedure of detection of Zn^{2+} and IO_3^-, different concentrations of Zn^{2+} and IO_3^- solution were added into the above Phen-QSR solution under the alkaline or acidic condition. The corresponding PL spectra were recorded. The relationships between Zn^{2+} or IO_3^- concentration and the PL intensity ratio of the QSR were plotted, and the calibration curves were established.

2.6 Detection of $Zn^{2+}$and IO_3^- in real samples

The fresh human blood samples were supplied from the hospital of Changchun China Japan Union Hospital. All the blood samples were mixed with acetonitrile (acetonitrile/blood was 1.5:1), then centrifuged at 10000 rpm for 10 min. The supernatant serum samples were obtained by eliminating large molecules and proteins. The serum samples were diluted to 2 times with PBS buffer before analysis, and different concentrations of Zn^{2+} were added to prepare the spiked samples. These serum samples were detected via the PL measurements under the optimal conditions. The table salt samples were purchased from local markets, and were dried at 120 ℃ for 6 h. Afterwards, sample solution was prepared by dissolving 10 g of table salt in 50 mL ultrapure water. The table salt samples were diluted to 2 times with PBS buffer, and different concentrations of IO_3^- were added to prepare the spiked samples.

3. Results and discussion

3.1 Characteristics of the QSR

In this work, the ratiometric PL sensor QSR was prepared via the formation of red-emitting QD@silica nanoparticles and the subsequent covalently linking of green-emitting QDs on the silica surface as shown in Scheme 1. The PL emission spectra of the green-emitting QDs, red-emitting QDs and the QSR were shown in Fig. 1. The green-emitting and red-emitting QDs

had emission maximum at 555 nm and 654 nm, respectively. The QSR exhibited a stable dual-emission PL spectrum (562 and 651 nm) under a single wavelength excitation. The PL emission peak of the green-emitting QDs had a slight red shift from 555nm to 562nm after linking on the silica surface. It indicated the surface state of the QDs was changed when chemically bonded on the silica surface. Meanwhile, larger volume and surface area of silica nanoparticles also leaded to the red shift of the PL emission peak.[30-31]

3.2 PL recovery and quenching of Phen-QSR system with Zn^{2+} and IO_3^-

The QSR had stable obvious dual-emission PL peak in the PBS buffer, as shown in Fig. 2 curve a. When Phen was introduced into the QSR system, there is a gradual attachment of Phen onto the QSR surface due to the affinity of the two nitrogen atoms of Phen with the surface Cd atoms of QDs. As a result, the PL intensity of green-emitting QDs was quenched, while the red PL from QDs in the silica nanoparticles kept stable. Phen quenched the PL of green-emitting QDs primarily by an electronic interaction rather than a "surface chemistry" interaction. Upon excitation, the photogenerated holes on the QDs preferentially transfered to the Phen ligands and became trapped, preventing the effective hole/electron recombination.[32] The relatively constant red PL served as internal reference to improve the sensitivity and reliability of the sensor. Fig. 2 curve b showed the PL intensity ratio (I_{562}/I_{651}) of QSR system decreased with the addition of Phen. Accordingly, the PL colors of the QSR solution changed from yellow to pale red under a UV lamp, which can be seen with the naked eye. It revealed that the QSR gradually emitted red PL of the inner QDs in the silica nanoparticles with the quenching of green-emitting QDs. Upon the addition of Zn^{2+}, the PL intensity ratio (I_{562}/I_{651}) of Phen-QSR system increased (curve c in Fig. 2), and the PL colors of the ratiometric solution changed to orange by naked eye under a UV lamp. It

was responsible for the fact that phen was dissociated from the surface of green-emitting QDs by Zn^{2+}, and soluble Zn-Phen chelate was formed in the solution. The electronic interaction between Phen and QDs was terminated, leading to the restoration of the PL intensity of QDs. When molar ratio of added Zn^{2+} and Phen was higher than 1:2, the PL intensity of green-emitting QDs cannot recover any more, suggesting that the chelating stoichiometric ratio of Zn^{2+} to Phen was 1:2. In order to verify the occurrence of chelating reaction rather than the influence of Zn^{2+} itself on the system, the PL intensity of the QSR was performed in the presence of Zn^{2+}. As shown in Fig. S1, Zn^{2+} itself did not affect the PL intensity ratio of QSR system in a wide range of concentrations, which demonstrated the chelating reaction between Zn^{2+} and Phen did take place. When IO_3^- was added into the Phen-QSR system under the acidic condition, IO_3^- can react with superficial green--emitting CdTe QDs, resulting in the further quenching of its PL intensity. The PL intensity ratio of QSR system subsequently decreased, as shown in Fig. 2 curve d. And the QSR solution changed from pale red to dark red under a UV lamp. The reaction mechanism expressed by the following equations: [33]

$$IO_3^- + 3CdTe\ QDs + 6H^+ \longrightarrow I^- + 3Te + 3Cd^{2+} + 3H_2O \qquad (1)$$

$$5I^- + IO_3^- + 6H^+ \longrightarrow 3I_2 + 3H_2O \qquad (2)$$

3.3 Optimum conditions for the detection of Zn^{2+} and IO_3^-

A series of experiments were performed to choose the optimize conditions for the detection of Zn^{2+} and IO_3^-. Fig. 3 showed the effect of Phen concentrations on the PL intensity ratio of QSR. Upon the addition of Phen, the PL intensity at 562 nm of the green-emitting QDs in QSR system was gradually decreased with the increasing of the Phen concentration. Correspondingly, the PL intensity ratio of the QSR decreased gradually. When Phen concentration was increased to be 200

μM, the PL intensity ratio (I_{562}/I_{651}) achieved minimum and kept stable. Therefore, 200 μM of Phen was used in the further experiments.

The pH value was of significant importance in the sensitive detection of Zn^{2+} and IO_3^-. So, we investigated the effect of pH on the PL quenching and recovering of the QSR system in the range of pH 4-9. QSR system was stable under weak acid or alkaline conditions. At low pH value (less than pH 4), QSR was etched by strong acid and the stability of the sensor greatly reduced. The results in Fig. 4A showed the PL intensity ratio of the Phen-QSR system with Zn^{2+} at the different pH. It can be seen that the maximum PL intensity ratio (I_{562}/I_{651}=3.11) of ratiometric system was obtained at pH 8. It indicated the chelation between Zn^{2+} and Phen can be easily occurred under the weak alkaline solution, and the PL intensity of the green-emitting QDs recovered obviously. However, strong basic environment can lead to the hydrolysis of Zn^{2+}, affecting the chelation reaction efficiency. Thus, we chose pH 8 PBS buffer for the detection of Zn^{2+}. The effect of pH on the PL intensity ratio of the Phen-QSR system with IO_3^- was displayed in Fig. 4B. It can be seen that under the alkaline condition (more than pH 7.5), IO_3^- hardly quenched the PL intensity of the green-emitting QDs on the surface of silica nanoparticles. And the quenching efficiency gradually increased with the increasing of the acidity in the range of pH 5.0-7.5, which indicated IO_3^- had strong oxidability under the acidic condition, and the oxidation-reduction reaction between IO_3^- and CdTe QDs can be performed.[34] Therefore, pH 5 was chosen in the further experiments for IO_3^- detection. In a word, Based on the modulation of pH, QSR system can effectively determine Zn^{2+} and IO_3^- under alkaline or acidic conditions, respectively.

The effect of reaction time on the QSR sensing system was also studied in this paper. For

this purpose, QSR and Phen were mixed according to the procedure described above for different time intervals. As shown in Fig. 5, the PL intensity ratio (I_{562}/I_{651}) rapidly decreased with the increase of reaction time, and reached minimum at 7 min. It indicated that the PL quenching of the green-emitting QDs was completed. When Zn^{2+} was added into the above solution, the PL intensity ratio of the ratiometric system increased with increasing reaction time and then kept constant over 6 min. Hence, 7 min and 6 min were chosen as the optimal reaction time for Phen quenching and Zn^{2+} detection. Fig. 6 showed the PL intensity ratio of the Phen-QSR system in the presence of IO_3^- as a function of incubation time. It can be seen that the PL of the green-emitting QDs continued to quench with the increase of the reaction time until 6 min, suggesting that the oxidation-reduction reactions between IO_3^- and CdTe QDs completed within 6 min. Based on the above results, we chosen 6 min as the optimal reaction time for the IO_3^- detection.

3.4 Detection of Zn^{2+} and IO_3^-

Under the optimum experimental conditions, the PL intensity ratio of Phen-QSR system was closely related to the concentration of Zn^{2+} and IO_3^-. Fig. 7A showed the PL intensity of the QSR at 562 nm increased gradually with the increasing concentration of Zn^{2+}. In the Fig. 7B, it was noticed that the PL intensity ratio (I_{562}/I_{651}) exhibited a linear response to the Zn^{2+} concentration. The linear range was from 5 to 100 μM, and a good linear correlation ($R^2 = 0.998$) was obtained. The linear regression equations were $I_{562}/I_{651} = 1.1526 + 0.0215\times$ C (Zn^{2+}), (μM). According to the IUPAC 3s criterion, the limit of detection (LOD=3σ/s) of Zn^{2+} was calculated to be 1.15 μM. Clearly, the distinguishable color changes of QSR solution from the pale red to pale yellow under UV lamp were obtained (Fig. 7C). As shown in Fig. 8, there was a linear relationship between the PL intensity ratio (I_{562}/I_{651}) of the Phen-QSR system and IO_3^- concentration in the range of 5-150

μM. The calibration curve can be expressed as I_{562}/I_{651} = 1.0242-0.0076× C (IO_3^-), (μM) and I_{562}/I_{651} = 0.7431-0.0018× C (IO_3^-), (μM). The correlation coefficients (R^2) were 0.997 and 0.998, respectively. The detection limit (LOD=3σ/s) for IO_3^- was 1.76 μM. As shown in Fig. 8C, the color of the probe solution changed from pale red to red under a UV lamp. The reaction could be clearly distinguished by naked eyes. A comparison of the present method and other methods in the linear range and detection limit were shown in Table S1. Compared with other sensors, our QSR system for Zn^{2+} and IO_3^- detection offered a comparable detection limit and dynamic range.

3.5 Interference study

In order to evaluate the selectivity of the nanosensor for Zn^{2+} and IO_3^-, the PL changes of the QSR system in the presence of various ions were investigated. Tolerable concentrations, the concentrations of foreign species causing less than ±5% relative error, were examined. As shown in Table S2, the tolerable concentration ratios of interference substances for Zn^{2+} detection was 500 fold for Na^+, K^+, Cl^-, NO_3^-, 200 fold for Mg^{2+}, SO_4^{2-}, Mn^{2+}, 50 fold for Ni^{2+}, Ba^{2+}, 10 fold for Fe^{3+}, Cd^{2+}, Cu^{2+}. Most of the interfering substances had little effect on the detection of Zn^{2+}. It can be seen from Table S3 that the tolerable concentration ratios of common interference ions and oxidant ions for IO_3^- dection was 500 fold for Na^+, K^+, Cl^-, 200 fold for Mg^{2+}, Mn^{2+}, NH_4^+, NO_3^-, SO_4^{2-}, 100 fold for CO_3^{2-}, HCO_3^-, CH_3COO^-, F^-, I^-, 5 fold for SO_3^{2-}, NO_2^-, O^{2-}. It indicated these interfering ions had little interference on IO_3^- detection. So the proposed ratiometric PL sensor for the detection of Zn^{2+} and IO_3^- had higher selectivity.

3.6 Detection of Zn^{2+} and IO_3^- in real samples

To evaluate the practicability of the QSR system, we detected Zn^{2+} and IO_3^- in human serum samples and table salt, respectively. All samples were prepared by spiking with Zn^{2+} and IO_3^- at

different concentration levels, respectively. During the determination of IO_3^- in table salt samples, in order to eliminate the influence of NaCl, 1mL of 3.4 M NaCl solution was added to make the work curve. The analytical results obtained by standard addition method were listed in Table 1 and Table 2. In order to evaluate the accuracy of the proposed method, the ICP method and UV spectrophotometry method were applied as reference standard methods for detection of Zn^{2+} and IO_3^-, respectively.[42-43] It can be seen that the found concentrations were in good agreement with that obtained by reference standard methods. The recoveries of the samples were in the range of 97-103%. The relative standard deviation (RSD) for three repeated measurements was less than 5%. The iodine contents of salt samples were accord with a standard level (iodine content label of the sample is 2250 μg/100g, and that is 17.7 μM before measurement). It indicated our QSR was feasible and reliability for real sample detection.

4. Conclusion

In conclusion, a novel dual-emission QD@silica nanoparticles-based ratiometric PL sensor for Zn^{2+} and IO_3^- has been developed. The red-emitting QDs encapsulated in the silica nanoparticle are inert to analyte, and the green-emitting QDs attached to the surface of the silica nanoparticles are specifically sensitive to analyte. Phen quenched the PL intensity of the green-emitting QDs. Then, Zn^{2+} can react with the Phen in the alkaline condition, resulting in the PL recovery of green-emitting QDs. IO_3^- can continue to quench the PL of green-emitting QDs in the acidic condition owing to the oxidation-reduction reaction between IO_3^- and QDs. Under optimum conditions, the pH-modulated sensor shows a detection limit 1.15 μM for Zn^{2+} and 1.76 μM for IO_3^-. The proposed QSR system exhibits the high sensitivity and selectivity to Zn^{2+} and IO_3^- and has been successfully used in the real analysis application with a simple, convenient,

facile procedure.

Acknowledgments

This work was financially supported by the National Natural Science Foundation of China (Nos.21275063 and 21005029), and the Youth Science Fund of Jilin Province (20140520081JH).

References

1 F. Wang, Z. Xie, H. Zhang, C. Y. Liu and Y. G. Zhang, *Adv. Funct. Mater.*, 2011, **21**, 1027−1031.

2 Y. Li, Q. Ma, Z. P. Liu, X. Y. Wang and X. G. Su, *Analytica Chimica Acta*, 2014, **840**, 68–74.

3 Q. Gan, X. Y. Lu, Y. Yuan, J. C. Qian and H. J. Zhou, *Biomaterials*, 2011, **32**, 1932-1942.

4 L. H. Jing, C. H. Yang and R. R. Qiao, *Chem. Mater.*, 2010, **22**, 420–427.

5 M. Xue, X. Wang, L. L. Duan, W. Gao, L. F. Ji and B. Tang, *Biosens Bioelectron*, 2012, **36**, 168-173.

6 Y. J. Gong, X. B. Zhang, C. C. Zhang, A. L. Luo, T. Fu, W. H. Tan, G. L. Shen and R. Q. Yu, *Anal. Chem.*, 2012, **84**, 10777−10784.

7 Z. X. Han, X. B. Zhang, L. Zhuo, Y. J. Gong, X. Y. Wu, J. Zhen and C. M. He, *Anal. Chem.*, 2010, **82**, 3108−3113.

8 C. F. Wu, B. Bull, K. Christensen and J. McNeill, *Angew. Chem. Int. Ed.*, 2009, **48**, 2741−2745.

9 D. W. Domaille, L. Zeng and C. J. Chang, *J. Am. Chem. Soc.*, 2010, **132**, 1194−1195.

10 J. Zhou, C. Fang, T. Chang, X. Liu and D. Shangguan, *J. Mater. Chem. B.*, 2013, **1**, 661−667.

11 C. Zong, K. Ai, G. Zhang, H. Li and L. Lu, *Anal. Chem.*, 2011, **83**, 3126-3132.

12 F. P. Yang, Q. Ma, Y. Wei and X. G. Su, *Talanta*, 2011, **84**, 411–415.

13 P. J. Fraker and L. E. King, *Annu. Rev. Nutr.*, 2004, **24**, 277–298.

14 W. C. Fischer and R. E. Black, *Annu. Rev. Nutr.*, 2004, **24**, 255–275.

15 P. A. Adlard and A. I. Bush, *J. Alzheimers Dis.*, 2006, **10**, 145–163.

16 A. M. H. Shabani, P. S. Ellis and I. D. McKelvie, *Food Chem.*, 2011, **129**, 704-707.

17 Y. X. Hou, L. P. Liu and Z. X. Du, *Physical Testing and Chemical Analysi*, 2011, **47**, 1262-3111.

18 T. L. Wang, S. Z. Zhao, C. H. Shen, J. Tang and D. Wang, *Food Chem.*, 2009, **112**, 215-220.

19 D. E. Benson, M. S. Wisz and H. W. Hellinga, *Curr Opin Biotechnol*, 1998, **9**, 370–376.

20 M. J. Ruedas-Rama and E. A. H. Hall, *Anal. Chem.*, 2008, **80**, 8260–8268.

21 G. Crivat, K. Kikuchi, T. Nagano, T. Priel, M. Hershfinkel, I. Sekler, N. Rosenzweig and Z. Rosenzweig, *Anal. Chem.*, 2006, **78**, 5799–5804.

22 Y. Chen, K. Y. Han and Y. Liu, *Bioorg Med Chem.*, 2007, **15**, 4537–4542.

23 Y. P. Shi, Z. H. Chen, X. Cheng, Y. Pan and C. Q. Yi, *Biosensors and Bioelectronics*, 2014, **61**, 397-403.

24 P. Kaleeswaran, I. A. Azath, V. Tharmaraj and K. Pitchumani, *Chempluschem*, 2014, **79**, 1361-1366.

25 Y. W. Huang, Q. Lin, J. M. Wu and N. Y. Fu, *Dyes and Pigments*, 2013, **99**, 699-704.

26 L. J. Tang, M. J. Cai, P. Zhou, J. Zhao and Y. J. Bian, *Journal of Luminescence*, 2014, **147**, 179-183.

27 Q. Ma, E. Ha, F. Yang and X. G. Su, *Analytica Chimica Acta*, 2011, **701**, 60–65.

28 K. Zhang, Q. S. Mei, G. J. Guan, B. H. Liu, S. H. Wang and Z. P. Zhang, *Anal.Chem.*, 2010, **82**, 9579−9586.

29 J. L. Yao, K. Zhang, H. J. Zhu, F. Ma, M. T. Sun and H. Yu, *Anal. Chem.*, 2013, **85**, 6461−6468.

30 Y. Q. Wang, Y. Y. Zhang, F. Zhang and W. Y. Li, *J. Mater. Chem.*, 2011, **21**, 6556-6562.

31 F. Vollmer, S. Arnold, D. Braun and I. Teraoka, *Biophysical Journal*, 2003, **85**, 1974–1979.

32 S. Banerjee, S. Kar and S. Santra, *Chem. Commun.*, 2008, **26**, 3037-3039.

33 M. Fan, L. Zhang and Q. L. Liu, *Journal of Analytical Science*, 2014, **30**, 16-20.

34 C. R. Tang, Z. H. Su, B. G. Lin, H. W. Huang and Y. L. Zeng, *Analytica Chimica Acta*, 2010, **678**, 203-207.

35 Z. P. Liu, G. Y. Li, Q. Ma and X. G. Su, *Microchim. Acta.*, 2014, **181**, 1385–1391.

36 Q. Ma, Z. H. Lin, N. Yang, Y. Li and X. G. Su, *Acta Biomaterialia*, 2013, **10**, 868–874.

37 H. Xu, Z. P. Wang, Y. Li, S. J. Ma and P. Y. Hu, *Analyst*, 2013, **138**, 2181-2191.

38 B. Haghighi, H. Hamidi and L. Gorton, *Electrochimica Acta.*, 2010, **55**, 4750-4757.

39 S. Abdollah, M. K. Hussein, H. Rahman and Z. Shiva, *ScienceDirect*, 2007, **52**, 6097-6105.

40 M. A. Tabrizi and L. Ebrahimi, *Journal of Electroanalytical Chemistry*, 2014, **724**, 8-14.

41 J. Jakmunee and K. Grudpan, *Analytica Chimica Acta*, 2001, **438**, 299-304.

42 Y. J. Li, W. T. Ma, J. H. Liu and E. R. Ma, *Chin. J. Prev. Med.*, 1997, **31**, 112-113.

43 G. N. P. Silva, A. Oliveira and E. A. Neves, *Revistas*, 1998, **9**, 171-174.

Captions:

Scheme 1 The schematic illustration of the QSR structure and the detection principle for Zn^{2+} and IO_3^-.

Fig. 1 The PL spectra of green-emitting QDs (a), red-emitting QDs (b) and QSR (c).

Fig. 2 The PL spectra of the QSR (a), QSR -200 μM Phen (b), QSR -200 μM Phen -100 μM Zn^{2+} (c), QSR- 200 μM Phen - 40 μM IO_3^-.

Fig. 3 The Effect of Phen concentration on the PL intensity ratios I_{562}/I_{651} of QSR. (a) 0 μM (b) 10 μM (c) 20 μM (d) 50 μM (e) 100 μM (f) 200 μM (g) 300 μM (h) 400 μM. Inset: the plot of the PL intensity ratios I_{562}/I_{651} of the ratiometric sensor toward Phen.

Fig. 4 (A) The effect of pH on the PL intensity ratios $I_{562}/I_{651}$of QSR with addition of 200 μM Phen and 100 μM Zn^{2+}, (B) The effect of pH on the PL intensity ratios $I_{562}/I_{651}$of QSR with addition of 200 μM Phen and 120 μM IO_3^-.

Fig. 5 The effect of the incubation time on the PL intensity ratios $I_{562}/I_{651}$of QSR with addition of 200 μM Phen(■) and subsequent 100 μM Zn^{2+} (●).

Fig. 6 The effect of the incubation time on the PL intensity ratios $I_{562}/I_{651}$of the QSR with addition of 200 μM Phen (■) and subsequent 120 μM IO_3^- (●).

Fig. 7 (A) The PL spectra of Phen-QSR with different Zn^{2+} concentrations from 0 to 100 μM. (a) 0 μM (b) 5 μM (c) 10 μM (d) 20 μM (e) 40 μM (f) 60 μM (g) 100 μM. (B) The linear plot of the PL intensity ratios I_{562}/I_{651} of QSR toward Zn^{2+}. (C) The photographs of the mix solution under UV lamp.

Fig. 8 (A) The PL spectra of Phen-QSR with different IO_3^- concentrations from 0 to 150 μM. (a) 0 μM (b) 5 μM (c) 10 μM (d) 20 μM (e) 30 μM (f) 50 μM (g) 80 μM (h) 100 μM (i) 130 μM (j) 150

μM. (B) The linear plot of the PL intensity ratios I_{562}/I_{651} of the ratiometric sensor toward IO_3^-. (C) The photographs of the mix solution under UV lamp.

Table 1 Determination of Zn^{2+} in human serum samples. A certain amount of human serum samples with different Zn^{2+} concentrations. (1) 20 μM (2) 40 μM (3) 60 μM.

Table 2 Determination of IO_3^- in table salts. A certain amount of table salts samples solution with different IO_3^- concentrations. (1) 20 μM (2) 40 μM (3) 60 μM.

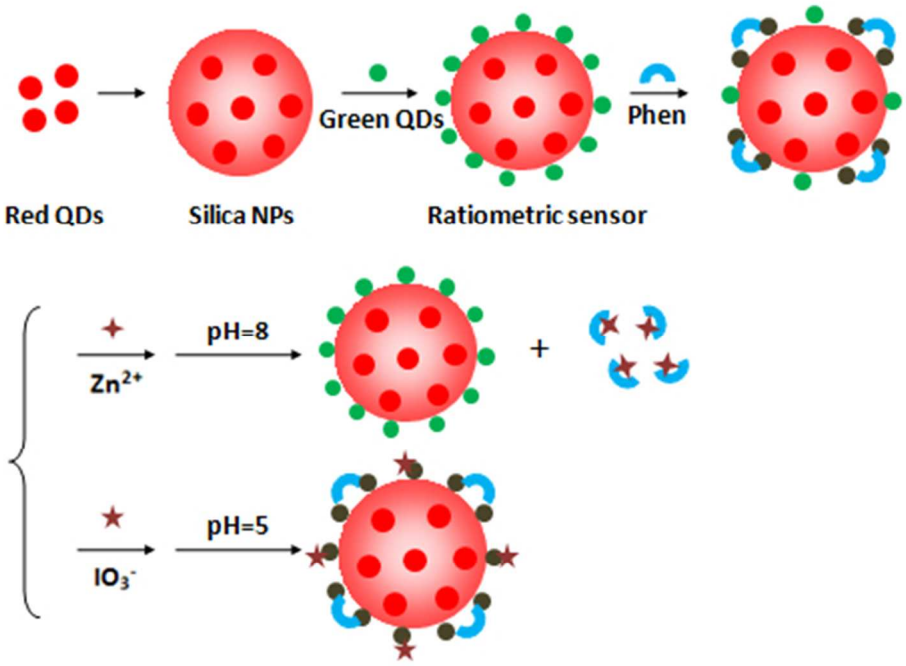

Scheme 1 The schematic illustration of the QSR structure and the detection principle for Zn2+ and IO3-.

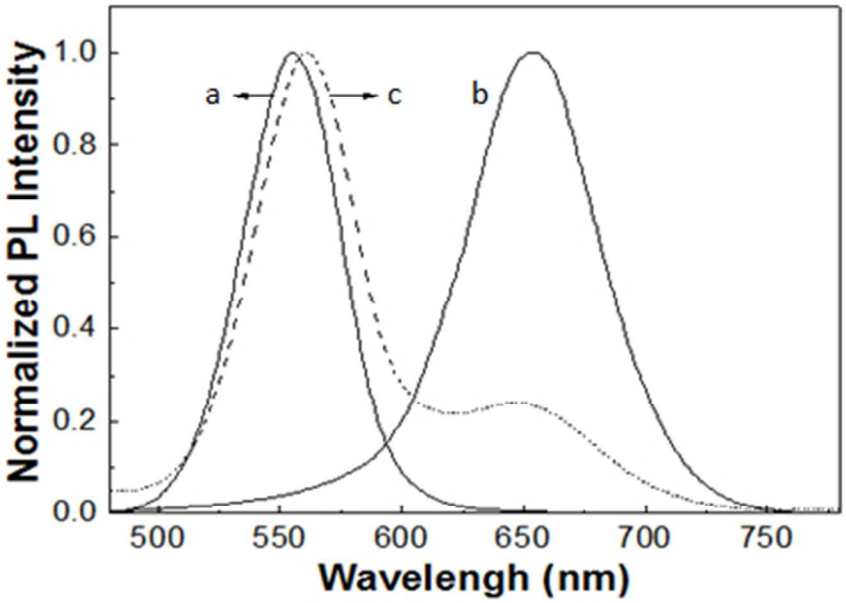

Fig. 1 The PL spectra of green-emitting QDs (a), red-emitting QDs (b) and QSR (c).

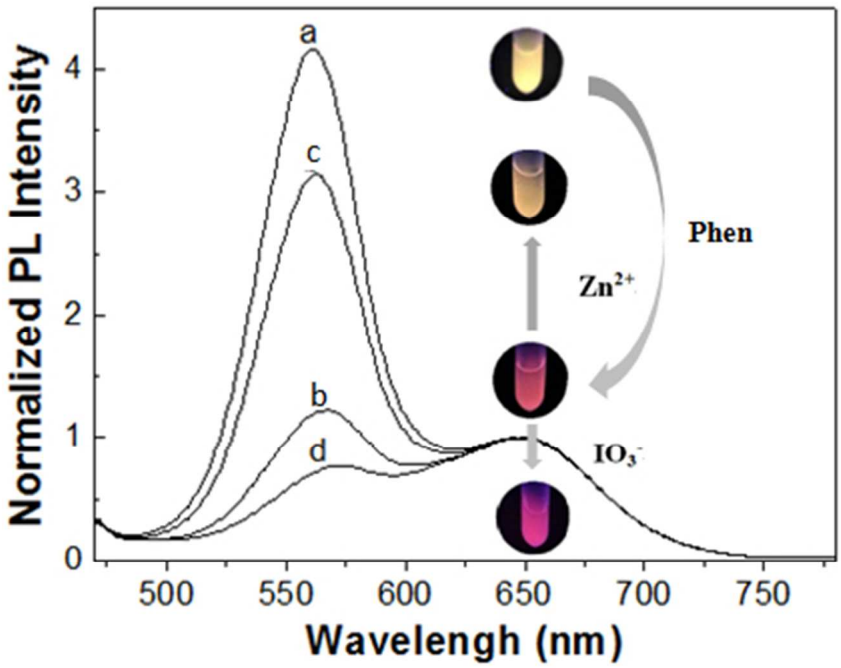

Fig. 2 The PL spectra of the QSR (a), QSR -200 μM Phen (b), QSR -200 μM Phen -100 μM Zn2+ (c), QSR-200 μM Phen - 40 μM IO3-.

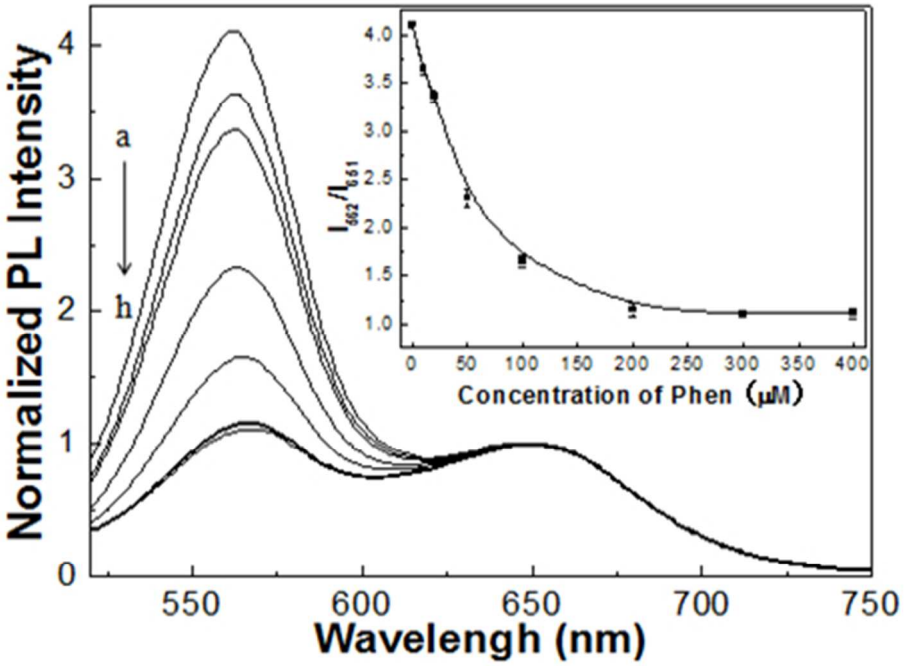

Fig. 3 The Effect of Phen concentration on the PL intensity ratios I562/I651 of QSR. (a) 0 μM (b) 10 μM (c) 20 μM (d) 50 μM (e) 100 μM (f) 200 μM (g) 300 μM (h) 400 μM. Inset: the plot of the PL intensity ratios I562/I651 of the ratiometric sensor toward Phen.

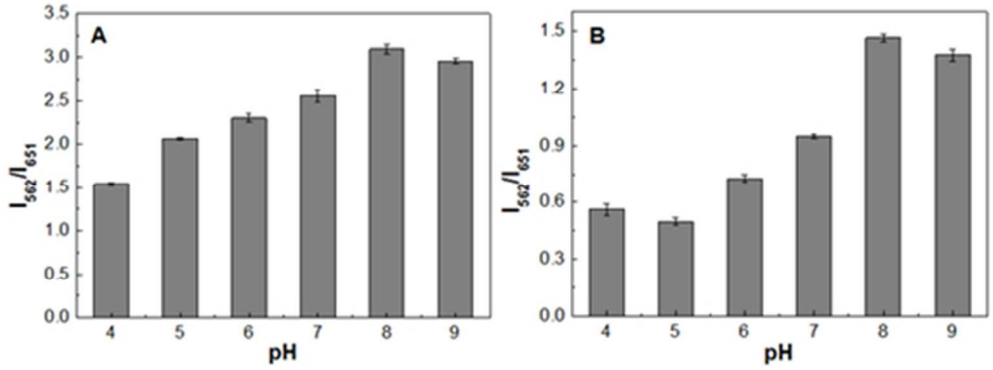

Fig. 4 (A) The effect of pH on the PL intensity ratios I562/I651of QSR with addition of 200 μM Phen and 100 μM Zn2+, (B) The effect of pH on the PL intensity ratios I562/I651of QSR with addition of 200 μM Phen and 120 μM IO3-.

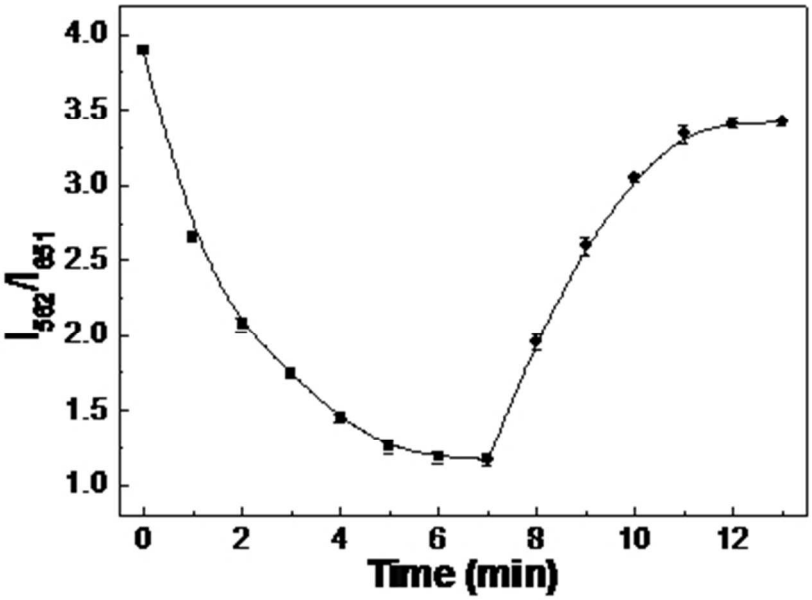

Fig. 5 The effect of the incubation time on the PL intensity ratios I562/I651of QSR with addition of 200 μM Phen(■) and subsequent 100 μM Zn2+ (●).

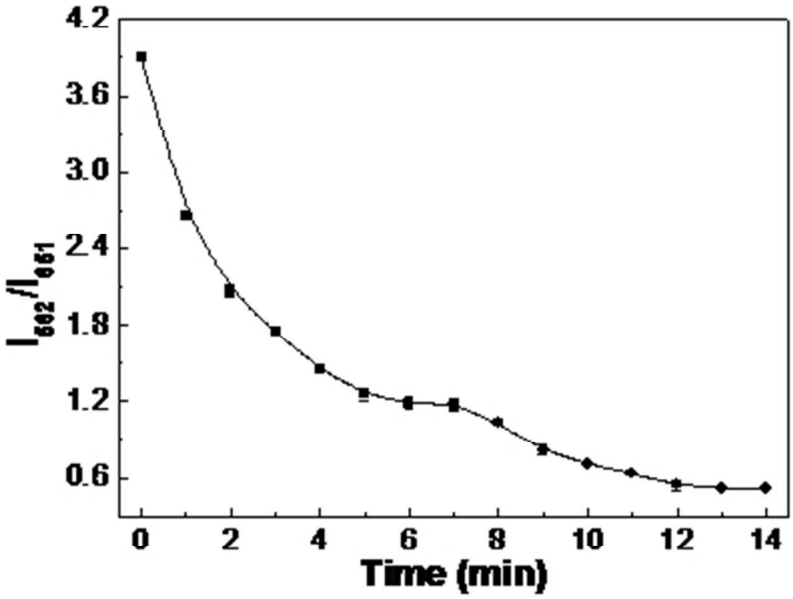

Fig. 6 The effect of the incubation time on the PL intensity ratios I562/I651of the QSR with addition of 200 μM Phen (■) and subsequent 120 μM IO3- (●).

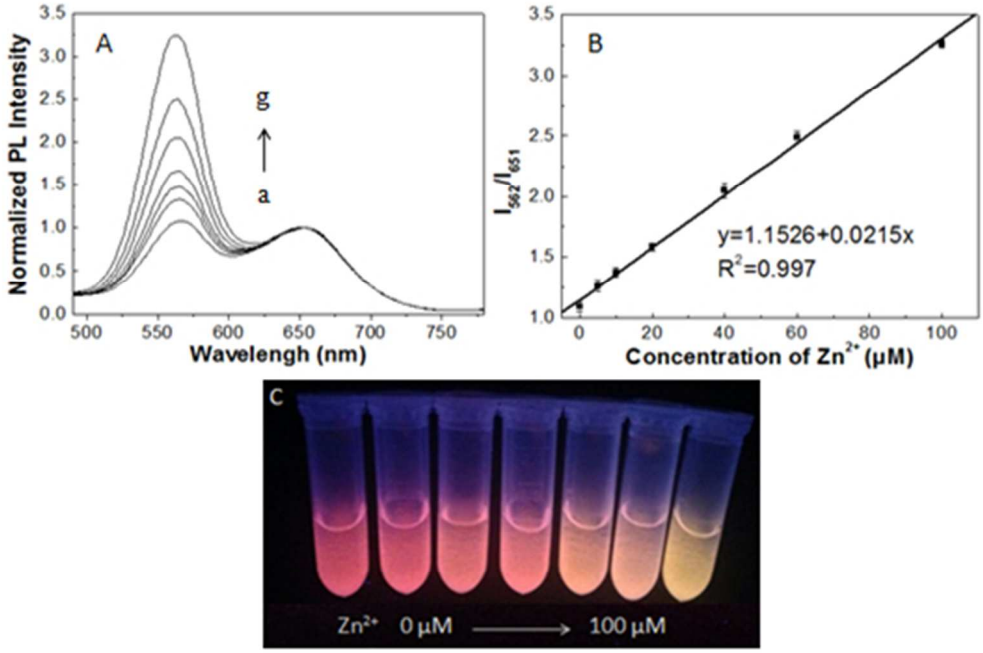

Fig. 7 (A) The PL spectra of Phen-QSR with different Zn2+ concentrations from 0 to 100 μM. (a) 0 μM (b) 5 μM (c) 10 μM (d) 20 μM (e) 40 μM (f) 60 μM (g) 100 μM. (B) The linear plot of the PL intensity ratios I562/I651 of QSR toward Zn2+. (C) The photographs of the mix solution under UV lamp.

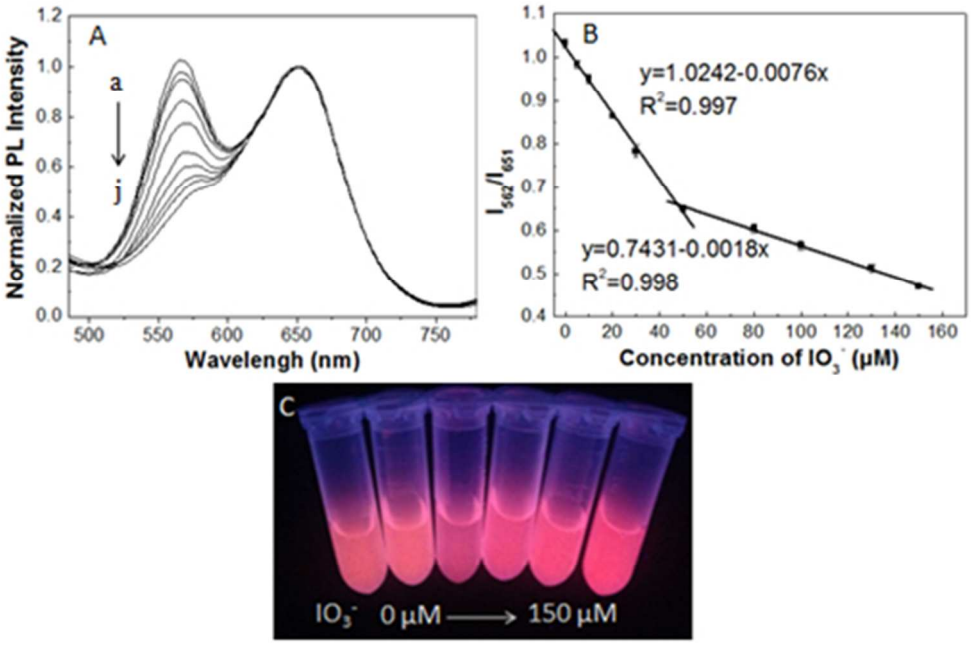

Fig. 8 (A) The PL spectra of Phen-QSR with different IO3- concentrations from 0 to 150 μM. (a) 0 μM (b) 5 μM (c) 10 μM (d) 20 μM (e) 30 μM (f) 50 μM (g) 80 μM (h) 100 μM (i) 130 μM (j) 150 μM. (B) The linear plot of the PL intensity ratios I562/I651 of the ratiometric sensor toward IO3-. (C) The photographs of the mix solution under UV lamp.

Table 1

Sample	Original (μM)	Added (μM)	Found (μM)		Recovery (%)	RSD (%, n=3)
			The proposed method	ICP		
1	6.82	20.00	26.40	26.21	97.90	3.73
2	7.35	40.00	47.81	48.42	101.15	2.28
3	7.54	60.00	67.16	67.59	99.37	1.65

Table 2

Sample	Original (μM)	Added (μM)	Found (μM)		Recovery (%)	RSD (%, n=3)
			The proposed method	UV spectrophotometry method		
1	18.52	20.00	39.05	38.46	102.65	2.85
2	22.37	40.00	61.41	62.81	97.60	2.71
3	20.83	60.00	81.39	81.95	100.93	1.69